

BCSJ Award Article

Evidence for Encaging Luminescent Guest Molecules in the Inner Cages of Zeolite Host

Tomoharu Kataoka,[1] Attila J. Mozer,[1] Yasunori Tsukahara,[1] Tomohisa Yamauchi,[1] and Yuji Wada*[1,2]

[1]Graduate School of Engineering, Osaka University, 2-1 Yamadaoka, Suita, Osaka 565-0871

[2]Department of Applied Chemistry, Graduate School of Science and Engineering, Tokyo Institute of Technology, 2-12-1 Ookayama, Meguro-ku, Tokyo 152-8552

Received June 29, 2007; E-mail: yuji-w@apc.titech.ac.jp

Clear evidence for encaging guest molecules in a host material was obtained for FAU-type zeolite containing fluorescein (FL) as a guest by employing the luminescence-quenching phenomenon of FL with C_{60}. Whereas fluorescence of FL molecules adsorbed on the outer surface of the zeolite was effectively quenched as well as that in a homogeneous solution, that of the most FL molecules in the cages of the zeolite did not suffer from quenching by C_{60}, giving clear evidence that FL molecules are located in the inner cages, which are inaccessible to C_{60}. Only the fluorescence of the FL molecules located in the cages in the outermost unit cells of the zeolite was partially quenched. This partial quenching can be understood by considering the structure of the zeolite and the critical distance of electron transfer inducing the fluorescence quenching.

Nanohybrid materials using host–guest systems are currently attractive for scientists working in chemistry and biology, because of their special properties and functions that cannot be obtained from independent constituents. To make use of these functions, optical functional materials based on nanohybrid systems have widely been studied, and a large number of papers on nanohybrid systems have been published.[1–8] Recently, our research group has reported that rare earth metal ions and a photosensitizer encaged in zeolite cages show rainbow-color photoluminescence.[9] The change in the color of the photoluminescence induced by changing the temperatures and the excitation wavelength is a good example of the special functions that cannot be obtained from independent constituents.

Distinction between guests encaged in hosts and those adsorbed on the surface of hosts is essential for systematizing nanohybrid chemistry. In order to systematize nanohybrid chemistry using host–guest systems, it is required to elucidate the origin of the specific properties of nanohybrid systems, which usually appear only when the guests are encaged into the hosts. NMR,[10–13] IR,[12,14,15] SEM,[16,17] optical microscopy,[18] and TEM[1,16,17,19] are used as the conventional methods for the distinction. NMR and IR are important tools that give information of local structures or environments of guests and hosts in the range from atomic size to molecular size. In studies on nanohybrid systems using organic host materials (e.g., cyclodextrin[20] or crown ether[21]), NMR and IR measurements provide us clear information on the position of guest molecules, because these organic hosts have small and simple structures compared to inorganic host materials (e.g., zeolite[9–15] or mesoporous silica[2,16]). Only partial information on the interaction for the nanohybrid systems containing inorganic hosts can be obtained by using these methods.

Although much discussion has been made on interactions between hosts and guests in studies on nanohybrid systems using inorganic host materials,[12–15] only a few reports can be found for distinction of guests encaged in hosts or adsorbed on the surface of hosts,[19,22,23] because it is difficult to determine clearly the guests' position by using conventional methods such as NMR,[10–13] IR,[12,14,15] SEM,[16,17] and optical microscopy.[18] Beutel and Su, for example, have measured NMR of an organic molecule (phenol) adsorbed onto FAU-type zeolite.[11] In their paper, the signal of hydroxy protons of phenol shifts from 0.7 to 1.3 ppm and that of H-atoms of the benzene ring shifts from 6.4 to 6.8 ppm due to adsorption on the zeolite surface. However, the location of the adsorption of phenol, either inner surface or outer surface of the zeolite, cannot be distinguished, because the chemical shift is derived from a similar interaction between organic molecules and both inner and outer surface of the zeolite, showing no difference between the two locations.

In the case of IR, Salavati-Niasari, for example, has reported the adsorption of a metal complex to FAU-type zeolite.[15] In this paper, the encapsulation of the metal complex into the zeolite was related to a shift in the IR bands (5–10 cm^{-1}) of the metal complex compared to solutions. This shift in the IR bands cannot give information on the location of the

Published on the web December 13, 2007; doi:10.1246/bcsj.80.2303

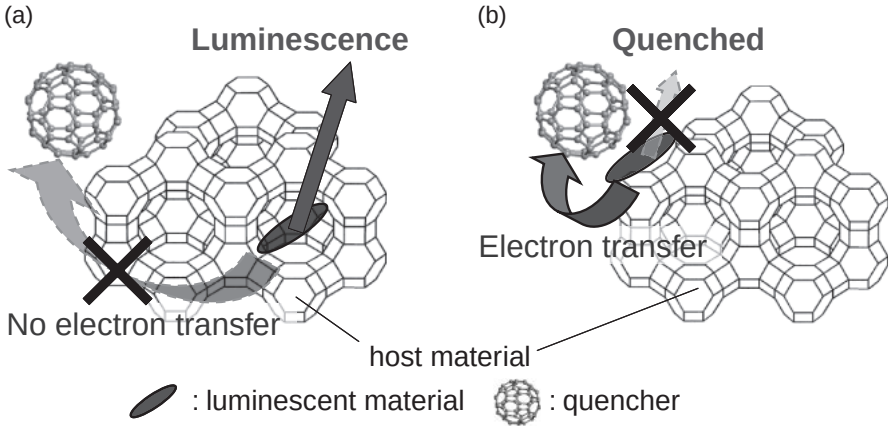

Fig. 1. Schematic image of the mechanism to distinguish the location of luminescent guest materials by quenching their luminescence. (a) In the case of a luminescent guest material locating inside the host material, luminescence is observed, whereas (b) in the case of a luminescent material adsorbed on the outer surface of host material, luminescence is quenched.

complex, that is, either adsorbed an inner surface or an outer surface, because the shift is induced by the interaction of the complex with the local structures of the surfaces.

SEM and optical microscopy measurements do not have magnification strength that made it possible to observe molecular-sized guests. This makes it difficult to use these techniques to distinguish clearly between guests encaged in the inside of hosts and those adsorbed on the outer surface of hosts.

TEM is a good method for observing nano-sized samples. In principle, TEM offers sufficient resolution power to observe structures at the single-molecule level. Unfortunately, this method requires specific techniques for preparing proper samples, and then, it can be troublesome when applied to complicated samples, such as nanohybrids. Damage to the samples from the electron beam should be also taken in account when nanohybrid systems containing organic molecules are investigated.

Based on the results from using the conventional methods for distinguishing the location of guests in hosts, it is significantly important and strongly desired in the field of nanohybrid systems to create a new method to identify the location of guests in hosts. In this paper, we report a new method for distinguishing the location of luminescent guests in hosts by employing a luminescence-quenching phenomenon. The theoretical background and the model systems based on the background follow.

Theoretical

Photoluminescence of a molecule is quenched when it is in solution with a quencher. However, when a luminescent guest is encaged in a host into which a quencher cannot penetrate, that is, a quencher cannot be in close proximity to a luminescent guest, then the luminescence of the guest is not quenched, resulting in no change in the photoluminescence intensity after adding the quencher molecules to the system (Fig. 1a). On the other hand, when a luminescent guest is adsorbed on the outer surface of a host, a quencher can approach the luminescent guest within the distance at which an electron transfer or energy transfer can proceed, and thus, the luminescence of the guest is effectively quenched (Fig. 1b). In order to realize this idea as a method for distinction of the locations of guests in the host, two requirements must be fulfilled. First, a luminescent guest should not come out from the inside of hosts. Second, a quencher should not invade into a host. It is worthy to note that the critical distance for electron transfer between a donor (a luminescent molecule) and an acceptor (a quencher) is several nanometers,[24,25] whereas that for energy transfer is about 10 nm for Förster relaxation[26] and 1 nm for Dexter relaxation.[27] In any case, the critical distances on the order of nanometers are considered to be proper for realizing the idea proposed here.

Model System

An experimental system was modeled by using FAU-type zeolite as a host material, fluorescein (FL) as a luminescent guest molecule, and fullerene (C_{60}) as a quencher. Nano-sized FAU-type zeolite (about 100 nm in diameter) is a suitable and attractive host material for optical applications due to its transparency and dispersibility in organic solvents. FAU-type zeolite has supercages of 1.3 nm internal diameters, which are connected to each other by 12-membered ring opening with 0.7 nm windows. FL as a luminescent guest molecule is one of the most famous and popular dyes having a molecular diameter of about 1.3 nm, which is a suitable size for encapsulation into the supercage of a FAU-type zeolite host. Then, once it is encaged into the supercage, FL cannot come out.

A large number of studies have been made on quenchers,[28] for example, halogens, metal cations, and paramagnetic gases. However, these quenchers are small molecules. Recently, many investigations have shown that fullerene (C_{60}) is a good electron acceptor. C_{60} is 0.8 nm in diameter, and this is larger than the window of FAU-type zeolite (0.7 nm). Therefore, C_{60} cannot enter into the zeolite. Furthermore, fluorescein–fullerene dyads have shown fluorescence quenching due to a photoinduced electron transfer from FL to fullerene (C_{60}) moiety,[29] indicating that C_{60} is an effective quencher of FL. Thus, C_{60} was selected as the quencher in the present work. This model should fulfill the two requirements mentioned in the theoretical background section.

Experimental

Materials. Tetramethylammonium hydroxide solution (10%

in water) and aluminum triisopropoxide powder were purchased from Kishida Chemical Co., Ltd. and Nacalai Tesque, Inc, respectively. LUDOX HS-40 colloidal silica (40 wt % suspension in water), fluorescein, and phthalic anhydride were purchased from Aldrich, and resorcinol was purchased from Wako Pure Chemical Industries, Ltd. Fullerene (C_{60}) was purchased from Tokyo Kasei Kogyo Co., Ltd. These reagents were used without further purification.

Nano-Sized FAU-Type Zeolite Synthesis. Synthesis of the nano-sized FAU-type zeolite was carried out according to a procedure reported in the literature.[30] Tetramethylammonium hydroxide aqueous solution (10% solution, 160.5 g) and deionized water (3.8 g) were added to aluminum isopropoxide (15 g), giving a clear solution. Then, silica sol (LUDOX HS-40, 24 g) was added, while stirring, and the mixture was further stirred for 30 min. The composition of this solution was $0.15Na_2O{:}5.5(TMA)_2O{:}2.3Al_2O_3{:}10SiO_2{:}570H_2O$. After 48 h of aging with stirring, the solution was heated at 373 K for 3 days. The resulting solid was separated by centrifugation (15000 G) for 1.5 h, and washed with deionized water. The solid was separated by centrifugation again and dried at 358 K.

Preparation of FL Encaged in Zeolite. FL encaged in the nano-sized zeolite was synthesized by the ship-in-bottle method reported in the literature.[31] Phthalic anhydride (200 mg) and resorcinol (297 mg) were mixed with the synthesized nano-sized FAU-type zeolite (500 mg), and the resulting white powder was heated up to 473 K under vacuum and kept at the temperature for 1 h. The obtained powder was washed by centrifugation and decantation with dichloromethane (twice) for removing the residual reactants and with ethanol (13 times) for removing FL from the outer surface of the zeolite, followed by drying at 353 K, resulting in the yellow powder (denoted as FL-NZ).

Preparation of the Sample of FL Adsorbed on the Outer Surface of the Zeolite. To prepare a sample with FL adsorbed on the outer surface of the zeolite, FL and the nano-sized zeolite were just mixed in ethanol for 12 h under stirring. In order to peel off the excess FL molecules, the sample was washed with pure ethanol and separated by centrifugation 10 times. The obtained yellow powder should contain only FL adsorbed onto the outer surface of the zeolite, because the size of FL is so large that it cannot enter into the zeolite through the window, which has a diameter of 0.7 nm. This sample is denoted as FL+NZ.

Measurements. The amounts of FL in the samples of FL-NZ and FL+NZ were calculated from the results of combustion chemical (C, H, and N) analysis by Perkin-Elmer CHNS Analyzer 2400.

In order to characterize FL-NZ and FL+NZ, absorption spectra and fluorescence spectra were measured on a JASCO V-570 spectrophotometer and on a Hitachi F-4500, respectively. FL-NZ ($0.33\ g\,L^{-1}$) or FL+NZ ($1.3\ g\,L^{-1}$) was dispersed into ethanol and put into a quartz optical cell for measuring absorption spectra and fluorescence spectra. The spectra of a FL solution (6.0×10^{-5} $mol\,L^{-1}$) were also measured.

For the fluorescence-quenching experiments of FL-NZ and FL+NZ, FL-NZ (0.15 g), or FL+NZ (0.28 g) was dispersed into 200 mL of mixed solvent of THF/ethanol (volume ratio, 2:1). The dispersions were transparent, but slightly turbid, indicating that the nano-sized zeolite particles were well dispersed in the solvents. C_{60} was dispersed into mixed solvent of THF/ethanol (volume ratio, 2:1). We judged that C_{60} was molecularly dispersed in these systems, because no precipitation occured in the resulting solutions. The C_{60} dispersion was added to the FL-NZ or FL+NZ dispersion (5 mL) in a quartz cell, giving the different concentrations of C_{60}, followed by the measurements of transmittance absorption spectra on a JASCO V-570 spectrophotometer and steady state front-face fluorescence spectra on a Hitachi F-4500. Absorption spectra of C_{60} in a solvent of THF/ethanol (volume ratio, 2:1) was also measured with different concentrations of C_{60} (0–$0.09\ g\,L^{-1}$).

Frequency Domain Lifetime Measurement. The fluorescence lifetimes of FL-NZ and FL+NZ were determined by using a frequency-domain method.[32] In this method, the excitation was performed by using an intensity-modulated light source. The modulation of the excitation light is given by b/a, where a is the average intensity and b is the peak-to-peak height of the incident light. The modulation of the emission is defined similarly as B/A, where A is the average intensity and B is the peak-to-peak height of the emission. The modulation of the emission is measured relative to the excitation, $m_\omega = (B/A)/(b/a)$, where ω is the modulation frequency in radians per a second. Although m_ω is actually a demodulation factor, it is usually called the modulation. Because of the time lag between absorption and emission, the emission is delayed in time relative to the modulated excitation. The delay is measured as a phase shift ϕ_ω between the excitation and emission. The lifetime of the sample can be calculated from the observed modulation (m_ω) and phase-shift (ϕ_ω). Since these values are affected by the equipments, the modulation and the phase-shift need to be corrected for unknown samples using a standard sample having a known lifetime. Single-, double-, and triple-exponential fitting were performed on the obtained data, and the χ^2 values which are the parameter for the goodness of the fitting between the obtained data and the calculated values, were compared. The fitting giving the smallest χ^2 value was employed to determine the lifetime therein.

The lifetime measurements were carried out on a Jobin Yvon SPEX Fluorog-3. A logarithmic sequence of 16 different frequencies, from 0.2 to 100 MHz, was applied to the Pockels cell.

First, we measured the lifetimes of an anthracene cyclohexane solution, a 2,5-diphenyloxazole (PPO) cyclohexane solution and a 1,4-bis[2-(5-phenyloxazolyl)]benzene (POPOP) ethanol solution in order to check the reliability of the lifetimes obtained by this method. The concentrations of these solutions were adjusted to show almost the same fluorescence intensity. The excitation wavelengths were 375, 340, and 345 nm, and the phase and modulation of the fluorescence were recorded at 420, 400, and 410 nm for each solution, respectively. An anthracene cyclohexane solution ($1.0 \times 10^{-5}\ mol\,L^{-1}$) with a lifetime of 4.10 ns[33] was used as a standard for correcting the modulation and the phase-shift. As a result, the lifetime of an anthracene cyclohexane solution was again found to be 4.03 ns (4.10 ns in the literature[33]), the lifetime of a PPO cyclohexane solution was found to be 1.41 ns (1.28 ns in the literature[33]), and the lifetime of a POPOP ethanol solution was found to be 1.10 ns (1.32 ns in the literature[33]) (see Fig. S1). These results confirmed the reliability of the frequency domain lifetime measurements carried out in this work.

For the lifetime measurements of FL-NZ and FL+NZ, a standard sample, which can be excited at the same excitation wavelength region as FL-NZ and FL+NZ and shows fluorescence at the same wavelength region, is required, because a photomultiplier tube possesses a wavelength-dependent time response affecting the frequency-domain lifetime measurements. A standard having a similar lifetime to FL-NZ and FL+NZ is also required. Thus, we selected a fluorescein ethanol solution (1.0×10^{-4} $mol\,L^{-1}$), which has a lifetime of 3.5 ns,[34] as the standard.

FL-NZ or FL+NZ was dispersed into ethanol, respectively, and these dispersions were introduced into a quartz cell for measuring. The amount of dispersed FL-NZ or FL+NZ was adjusted to show almost the same fluorescence intensity as the standard solution. The excitation wavelength was 400 nm, and the phase and modulation of the fluorescence were recorded at 510 nm.

Results

Sample Preparations. We employed a ship-in-bottle synthesis method[31] for preparing FL encaged in a nano-sized zeolite host (FL-NZ). Fluorescein can be prepared by reacting phthalic anhydride with resorcinol in the presence of zinc chloride as a Lewis acid catalyst.[35] Scaiano et al. have reported the ship-in-bottle synthesis of FL in an FAU-type zeolite host, in which the zeolite worked as an acid catalyst according to their paper.[31] In their paper, FAU-type zeolite (CsY), which is usually regarded as a weak acidic catalyst or even as a basic one, works as an acid catalyst for the synthesis of FL. In our study, we used the nano-sized FAU-type zeolite synthesized in our lab, which contained tetramethylammonium (TMA) cations and Na cations as the exchanged cations. Although this zeolite should have a weak acidity, it would behave as an acid catalyst in this reaction as well as in the reaction using zeolite CsY by Scaiano et al.

In the ship-in-bottle synthesis carried out in our work, FL should have been synthesized both inside the cavity and on the outer surface of the zeolite. Thus, in order to remove FL synthesized on the outer surface, the zeolite powder was washed thoroughly after heat treatment. The color of the extracted solvent was deep yellow until the eighth wash, and it changed gradually to transparent pale yellow by the further washing of 5 times. We judged that most of the FL molecules on the outer surface were removed and the residual FL molecules should not affect the optical measurements in the experiments carried out in the work. This was confirmed with the results of the lifetime measurements of the fluorescence as mentioned below.

From the results of the combustion chemical (C, H, and N) analysis of the FL-NZ and FL+NZ, the amounts of FL incorporated into the zeolite were calculated. The result of the analysis of FL-NZ was found to be C, 5.63; H, 3.50; N, 0.93 wt %. Based on the assumptions that 1) the nitrogen is from TMA cations, and 2) the chemical formula of the unit cell of the zeolite is $Na_xAl_{58}Si_{134}O_{384}$ (x = from 0 to 40), which is a conventional chemical formula of a zeolite X, the amount of FL incorporated into the zeolite in FL-NZ was calculated to be 3.4 wt %, corresponding to 1.3 molecules to 1.4 in a unit cell. The result of the analysis of FL+NZ was found to be C, 4.58; H, 3.28; N, 1.25 wt %. Based on the same assumptions mentioned above, the amount of FL adsorbed on the outer surface of the zeolite was calculated to be 0.41 wt %.

Characterization of FL-NZ and FL+NZ. The absorption spectra and the fluorescence spectra of the dispersion systems of FL-NZ and FL+NZ in ethanol were measured and compared to those of FL in ethanol as shown in Fig. 2. FL in ethanol showed two absorption peaks at 456 and 482 nm (Fig. 2a, solid line) and fluorescence peaks at 512 and 540 nm (Fig. 2a, gray line). Anpo et al. have reported that FL in ethanol shows two absorption peaks at 450 and 485 nm and by a fluorescence peak at 515 nm with a shoulder around 550 nm.[36] The excitation spectrum monitored at 505 nm in the fluorescence showed two peaks at 456 and 482 nm (Fig. 2a, dashed line), showing a similar shape to the absorption spectrum but a different peak intensity ratio.

FL-NZ showed an absorption peak at 455 nm (Fig. 2b, solid line). The steep background was due to the light scattering by the dispersed zeolite particles. In comparison with the FL solution, the peak corresponding to that at 482 nm of the FL solution disappeared in FL-NZ. A similar spectrum has been reported in the literature,[31] showing an absorption peak at 450 nm for FL in zeolite. The average concentration of FL contained in the dispersion of FL-NZ was estimated to be 1.3×10^{-5} mol L^{-1} using the absorption coefficient at 456 nm obtained by the absorption measurements of the FL solution, although the FL molecules were located in the cages of the zeolite. The concentration of FL estimated from the absorption spectrum was half of that estimated from the amount of FL molecules contained in the zeolite determined from the elemental analysis of FL-NZ (3.3×10^{-5} mol L^{-1}). The difference between the average concentration estimated from the absorption spectrum and that determined from the elemental analysis is probably due to the estimation using the absorption coefficient determined for the FL solution, in spite of the FL molecules being located in the cages of the zeolite. The absorption coefficient for FL in the cages of the zeolite might be changed from that for FL solution by encaging the molecules. Fluorescence spectrum of FL-NZ is shown in Fig. 2b by a gray line, exhibiting a fluorescence peak at 515 nm. This spectrum is similar with the spectrum of FL in FAU-type zeolite reported by Scaiano et al.[31] It is also very similar to that of the FL solution, suggesting that FL molecules in the zeolite cavity are isolated in the environment similar to that in ethanol. The excitation spectrum observed for the FL-NZ dispersion showed a peak at 465 nm with a shoulder at 450 nm, which were slightly shifted to blue compared to those observed for the FL solution (Fig. 2b, dashed line). Then, these spectra have confirmed successful synthesis of fluorescein molecules in the zeolite cavity.

In the case of FL+NZ, an absorption peak and an excitation peak (monitored at 505 nm fluorescence) were observed at the same wavelength of 448 nm (Fig. 2c, solid line), which was slightly shifted from that of the FL solution and that of FL-NZ to the shorter wavelength. The average concentration of FL contained in the dispersion of FL+NZ was estimated to be 1.36×10^{-5} mol dm^{-3} using the absorption coefficient at 456 nm obtained by the absorption measurements of the FL solution, and the FL molecules were located on the outer surface of the zeolite. The concentration is close to that estimated from the amount of FL molecules contained in the zeolite determined from the elemental analysis of FL+NZ (1.66×10^{-5} mol dm^{-3}).

A fluorescence peak was observed at 513 nm with a shoulder at 540 nm (Fig. 2c, gray line). The excitation spectra showed a peak at 448 nm with a weak shoulder around 480 nm. Whereas the two peaks were observed in the excitation spectra of the FL solution, only one peak was distinguished in that of FL+NZ. The second peak observed at the longer wavelength for the solution was weak, resulting in a weak shoulder observed in the spectrum of FL+NZ. The similar

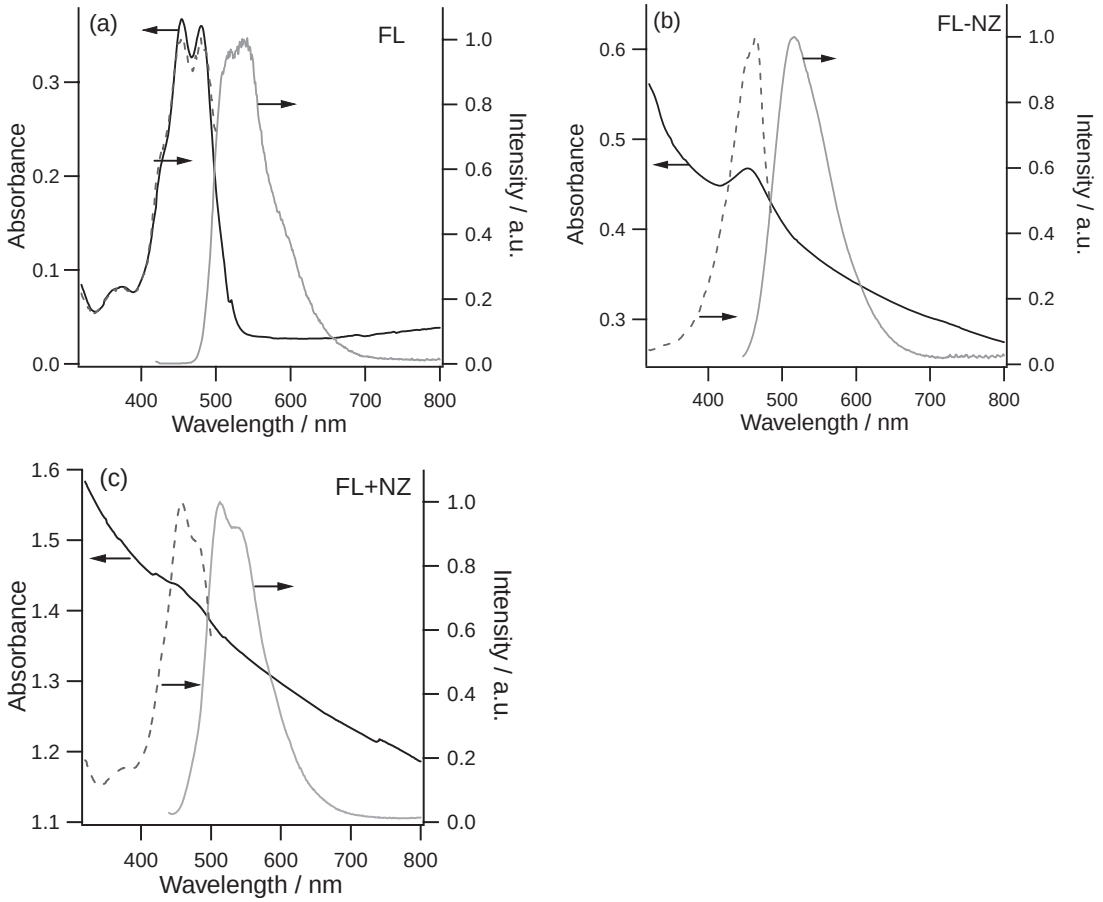

Fig. 2. Absorption (black solid line), photoluminescence (excited at 400 nm) (gray solid line), and excitation (monitored at 505 nm) (dashed line) spectra of (a) FL solution (6.0×10^{-5} mol dm^{-3}), (b) FL-NZ dispersion (0.33 g dm^{-3}), and (c) FL+NZ dispersion (1.3 g dm^{-3}) in ethanol.

shapes in the absorption spectrum and the fluorescence spectrum observed for FL+NZ to those observed for the FL solution and FL-NZ indicate that FL molecules adsorbed on the outer surface of the zeolite should be present in a similar environment to those of the solution and the FL-NZ dispersion. The only difference between FL-NZ and FL+NZ must be the location of FL molecules, i.e., in the cage or on the outer surface. Summarizing the characterization of FL-NZ and FL+NZ by observing the absorption and fluorescence, these photophysical properties should be insensitive to the location of the FL molecules, making it difficult to distinguish the locations of the molecules.

Fluorescence Lifetime. The results of the frequency domain lifetime measurements are shown in Fig. 3. The modulation (m_ω) and the phase shift (ϕ_ω) are denoted by open squares and open triangles, respectively, in the top panels. Single-, double-, and triple-exponential fitting were performed on the data shown in the top panels of Fig. 3 for FL-NZ and FL+NZ. The values of χ^2 were compared for the three fittings of each sample. In FL-NZ, the χ^2 values for the single-, double-, and triple-exponential fitting were 9.72, 7.94, and 3.50, respectively (Table 1), and the triple-exponential fitting gave the lowest χ^2 value. The result of the triple-exponential fitting is plotted in the top left panel of Fig. 3 as the dashed line, and the residuals in the fitting compared to the experimental data are shown in the bottom left panel of Fig. 3. In the result of the triple-exponential fitting, the three lifetimes were obtained to be $\tau_1 = 1.5$ ns, $\tau_2 = 0.0$ ns, and $\tau_3 = 9930$ ns. The component of τ_2 (=0.0 ns) was due to the scattered light from the zeolite, and the component of τ_3 (=9930 ns) was neglected because of its low fraction ($\alpha_3 = 0.03$). Therefore, the fluorescence lifetime of FL-NZ was determined to be 1.5 ns. Only one component of the fluorescence lifetime determined for FL-NZ indicates that the FL molecules are in a homogeneous environment, i.e., in the cavity of the zeolite, which means that the amount of FL remaining on the outer surface of the zeolite is negligible.

The result of the triple-exponential fitting for FL+NZ is shown in the top right panel of Fig. 3 as a dashed line, and the residuals in the fitting are shown in the bottom right panel in Fig 3. In FL+NZ, the χ^2 values for the single-, double-, and triple-exponential fitting were 10.03, 8.87, and 3.56, respectively (Table 1), and the triple-exponential fitting gave the lowest χ^2 value again. From the triple-exponential fitting, three lifetimes were calculated to be $\tau_1 = 3.0$ ns, $\tau_2 = 0.0$ ns, and $\tau_3 = 1124$ ns. The component of τ_2 (=0.0 ns) was due to the scattered light from the zeolite, and the component of τ_3 (=1124 ns) was neglected, because of its low fraction ($\alpha_3 = 0.05$) again. Therefore, the fluorescence lifetime of FL+NZ was determined to be 3.0 ns.

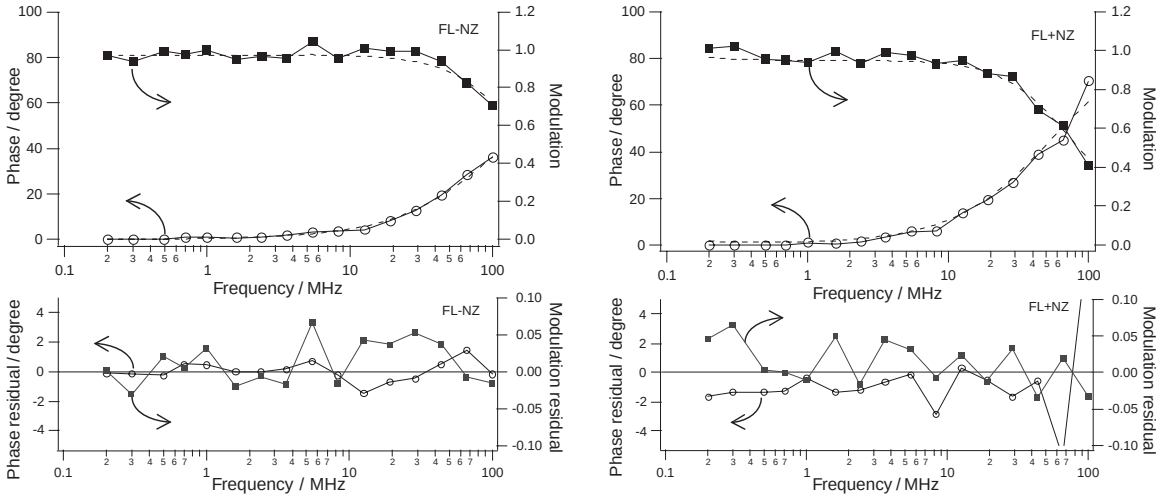

Fig. 3. Frequency domain lifetime plots for FL-NZ ($\tau = 1.5$ ns) (left panels) and FL+NZ ($\tau = 3.0$ ns) (right panels) of the ethanol dispersions. The dashed lines in the top panels are the results of fitting, and the residuals in the fitting are shown in the bottom panels, in which phase residuals are shown by circles and modulation residuals are shown by squares, respectively. The FL-NZ and FL+NZ dispersion were excited at 400 nm, and the fluorescent intensities of the samples were monitored at 510 nm.

Table 1. Fluorescence Lifetimes of FL, FL-NZ, and FL+NZ in Ethanol[a)]

		Lifetime/ns			Pre-exponential factors			
Samples	Fitting	τ_1	τ_2	τ_3	α_1	α_2	α_3	χ^2
FL		3.5[b)]	—	—	1	—	—	—
FL-NZ	one-component	1.4	—	—	1	—	—	9.72
	two-component	1.6	0.0	—	0.81	0.19	—	7.94
	three-component	1.5	0.0	9930	0.85	0.11	0.03	3.50
FL+NZ	one-component	3.4	—	—	1	—	—	10.03
	two-component	3.7	0.0	—	0.88	0.12	—	8.87
	three-component	3.0	0.0	1124	0.94	0.01	0.05	3.56

a) The excitation wavelength was 400 nm, and the phase and modulation of the fluorescence were recorded at 510 nm. b) From Ref. 34.

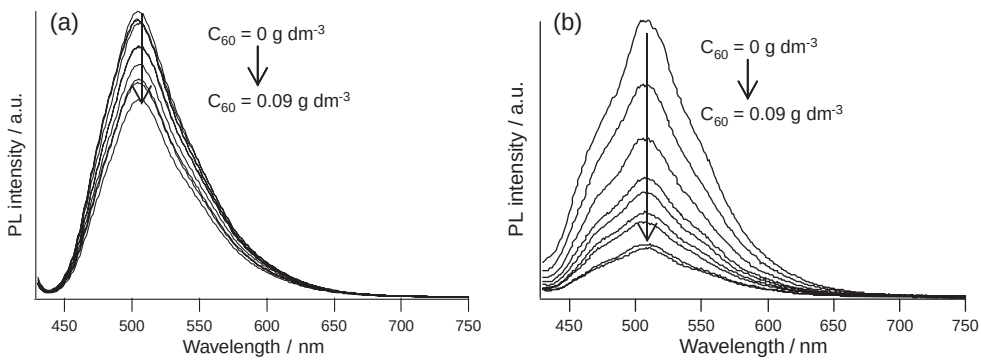

Fig. 4. Fluorescence quenching (excited at 420 nm) of (a) FL-NZ dispersion and (b) FL+NZ dispersion at various C_{60} concentrations (solvent: THF/ethanol, volume ratio = 2:1).

The lifetime for FL-NZ (1.5 ns) was shorter than that in ethanol solution, and the lifetime for FL+NZ was closed to that in ethanol solution. The shorter lifetime for FL-NZ compared to that of FL or FL+NZ can be attributed to an encapsulating effect of the zeolite host.

Fluorescence Quenching. In Fig. 4, fluorescence-quenching phenomena of FL-NZ and FL+NZ were examined by the addition of C_{60} into the dispersions. We examined the quenching phenomena with variety of C_{60} concentrations (from 0 to 0.09 g dm^{-3}). Figure 4 shows fluorescence quenching of FL-NZ and FL+NZ, in which fluorescence of FL+NZ was effectively quenched compared to that of FL-NZ. Detailed analysis of the quenching phenomena is discussed in the following section.

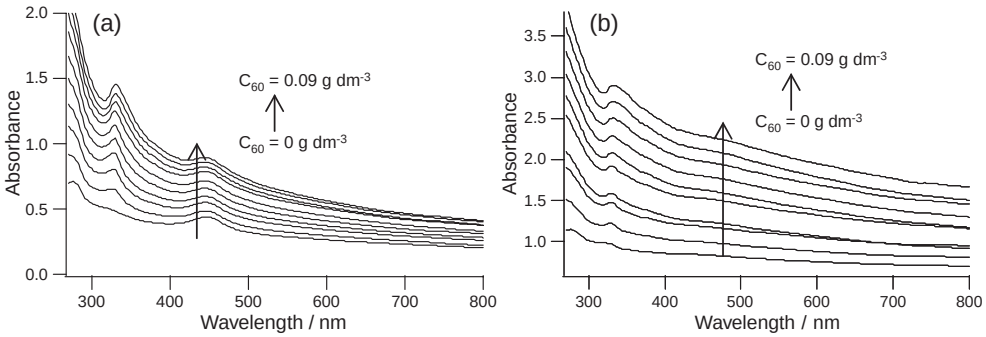

Fig. 5. Absorption spectra of (a) FL-NZ dispersion and (b) FL+NZ dispersion for various C_{60} concentrations (solvent: THF/ethanol, volume ratio = 2:1).

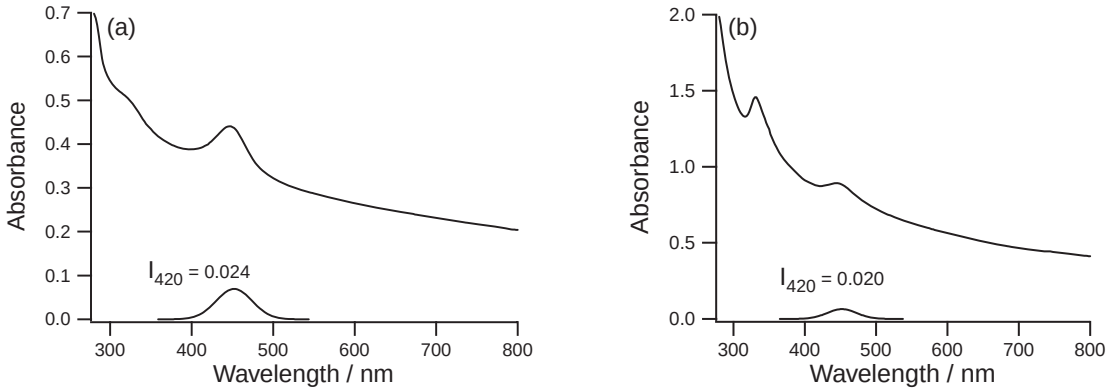

Fig. 6. Absorption spectra of FL-NZ dispersion (a) without C_{60} and (b) in the presence of 0.09 g dm^{-3} of C_{60} (solvent: THF/ethanol, volume ratio = 2:1). The curves shown on the horizontal axises are the intrinsic absorption spectra of only FL obtained by subtracting the background from the observed spectra.

Discussion

Shading Effect. The absorption spectra of the FL-NZ (in (a)) dispersion and the FL+NZ dispersion (in (b)) containing C_{60} at various concentrations are shown in Fig. 5. The absorption by FL was observed on the broad baseline at 455 and 458 nm, for FL-NZ and FL+NZ, respectively. The baseline resulted partially from the light scattering by the zeolite particles. Furthermore, the baseline gradually increased with an increase in the amount of added C_{60} due to the broad absorption of C_{60} ranging in the whole wavelength scale as shown in Fig. 5 (See also absorption spectra of C_{60} dispersions at various concentrations shown in Fig. S2.). These spectra show an important fact that C_{60} absorbs the excitation light for FL (420 nm), and the photon number in light for exciting FL should be decreased by this absorption (shading effect). Thus, we needed to correct the fluorescence spectra (Fig. 4) showing quenching by adding C_{60} in order to discussing the intrinsic quenching phenomena.

Figure 6 shows the absorption spectra of the FL-NZ dispersion in the presence of C_{60} and its absence. The intrinsic absorption spectrum of only FL can be obtained by subtracting the background attributed to the light scattering by the zeolite particles and the absorption of C_{60} from the observed spectrum, giving the curves shown on the horizontal axises of the figures. In the case of FL-NZ, the absorbance of FL at 420 nm was determined to be 0.024 without C_{60} (Fig. 6a). However, the intrinsic absorbance of FL at 420 nm was determined to be 0.020 in the presence of 0.09 g dm^{-3} of C_{60} (Fig. 6b). Thus, it can be concluded that the absorbed light intensity at the excitation wavelength (420 nm) of FL in FL-NZ in the presence of 0.09 g dm^{-3} of C_{60} decreases to 82% compared to that of FL in FL-NZ without C_{60}. Then, it should be noted that the decreases in the fluorescence intensity observed for the dispersions containing FL-NZ and FL+NZ by adding C_{60} in Fig. 4 are partially due to the decrease in the light intensity absorbed by FL.

Here, we estimated the shading effect supposing that the shading effect is in proportion to the concentrations of C_{60}, and corrected the fluorescent spectra shown in Fig. 4, which are shown in Fig. 7. For example, the absorbed light intensity due to FL-NZ at the excitation wavelength by FL-NZ with 0.09 g dm^{-3} of C_{60} was 82% compared to that by FL-NZ without C_{60}. If FL-NZ in the presence of 0.09 g dm^{-3} of C_{60} could absorb the same intensity as FL-NZ without C_{60}, it would show stronger fluorescence by 1.22 times (=1/0.82 times). Taking the shading effect into consideration as described above, the fluorescence spectra of FL-NZ and FL+NZ with various concentrations of C_{60} were corrected and are shown in Fig. 7.

Now, we can discuss the quenching effects of C_{60} on the fluorescence of FL molecules present in the cage and on the outer surface of the zeolite. In the case of the FL-NZ dispersion, the intensity of fluorescence from FL encaged in a zeolite cage was quenched by 13% when 0.09 g dm^{-3} of C_{60} was added (Fig. 7a). On the other hand, the fluorescence intensities

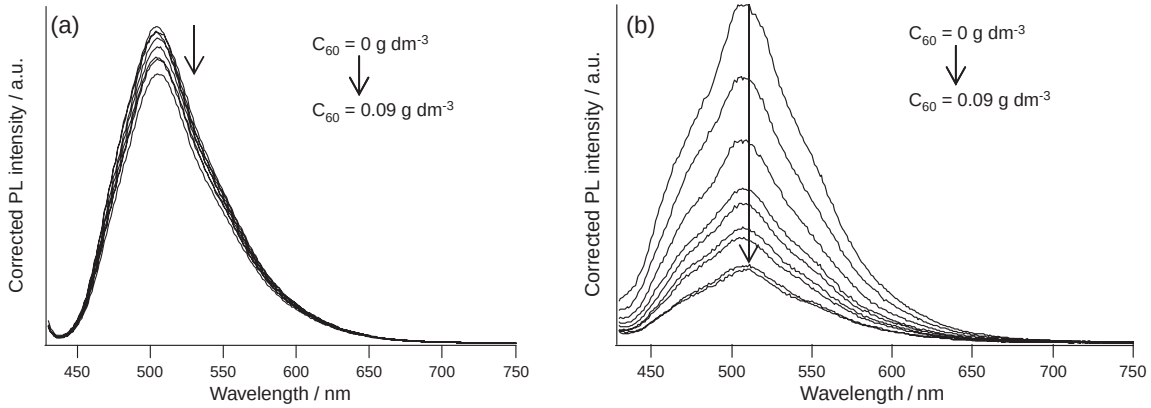

Fig. 7. Fluorescence quenching of (a) FL-NZ dispersion and (b) FL+NZ dispersion for various C_{60} concentrations after correction considering the shading effect by C_{60}.

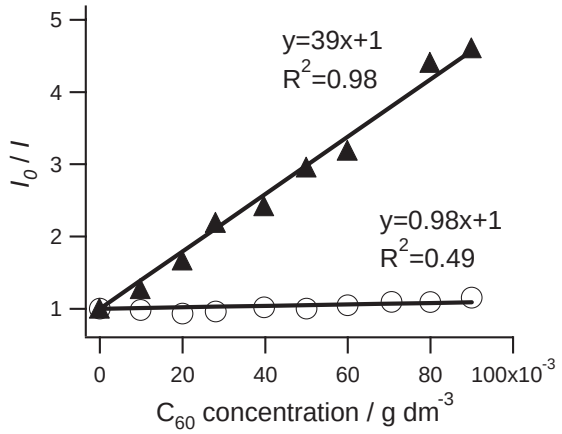

Fig. 8. Stern–Volmer plots for FL-NZ (open circle) and FL+NZ (closed triangle) with varied C_{60} concentrations.

from FL were effectively decreased by 77% by adding the C_{60} in the case of FL+NZ (Fig. 7b). The difference of the quenching phenomena between FL-NZ and FL+NZ is clearly demonstrated in these figures, i.e., the drastic decrease in the fluorescence intensity was observed for the FL+NZ dispersion, but only a little quenching occurred with the FL-NZ dispersion. This difference can be used to provide evidence for the location of FL molecules in the zeolite cage as discussed in the following section.

Stern–Volmer Plot. Although it is not appropriate to carry out a Stern–Volmer plot for the data shown in Fig. 7 without considering the heterogeneous location and distribution of FL molecules in the dispersion systems, we prepared one in order to further discussion of these systems. Figure 8 shows Stern–Volmer plots for the FL-NZ and FL+NZ dispersions in the presence different concentrations of C_{60}. The two plots for the FL-NZ and FL+NZ dispersions are demonstrated the apparent linearity. But this apparent linearity should give us a key for understanding the quenching phenomena occurring in these systems by analyzing as described below.

The slope of the Stern–Volmer plot (K_{SV}) can be related to the rate constant of the quenching process in the Stern–Volmer relation:[37]

$$\frac{I_0}{I} = 1 + K_{SV}[Q] = 1 + \tau k_q[Q], \quad (1)$$

Table 2. Slopes of Stern–Volmer Plots (K_{SV}), Fluorescence Lifetimes (τ), and Quenching Rate Constants (k_q) for FL, FL-NZ, and FL+NZ

Sample	K_{SV}/dm^3 g^{-1}	τ/ns	k_q/dm^{-3} g ns^{-1}
FL	4.6	3.5[a)]	1.3
FL-NZ	0.98	1.5	0.65
FL+NZ	39	3.0	13

a) From Ref. 34.

where I_0 and I represent the fluorescence intensity of the luminescent materials in the absence and in the presence of quencher, respectively, $[Q]$ is the quencher concentration, τ is the fluorescent lifetime in the absence of quencher, and k_q is the rate constant for a quenching process. The slopes of Stern–Volmer plot (K_{SV}) were found to be 0.98 dm^3 g^{-1} for the FL-NZ dispersion and 39 dm^3 g^{-1} for the FL+NZ system. The quenching rate constants (k_q) were calculated from the Eq. 1 using the values of K_{SV} and τ in Table 2. The k_q value for the FL-NZ dispersion was obtained to be 0.65 dm^{-3} g ns^{-1}, whereas it was found to be 13 dm^{-3} g ns^{-1} in the case of FL+NZ, which is 20 times larger than that for FL-NZ.

The k_q value was also determined for the solution of FL. Figure S3 in the Supporting Information shows the absorption of an FL solution in the absence and the presence of C_{60} in the various amounts. The fluorescence spectra were measured for the same solutions as employed in the experiments of Fig. S3 (Fig. S4). The fluorescence spectra showing the quenching effects were corrected considering the shading effect in the same method as described above (Fig. S5). The value of K_{SV} was determined by carrying out the Stern–Volmer plots from the results of the fluorescence spectra corrected by considering the shading effects (Fig. S6). The K_{SV} was found to be 4.6 dm^3 g^{-1}, giving a k_q of 1.3 dm^{-3} g ns^{-1} (Table 2).

The k_q values obtained from the Stern–Volmer plots for the dispersions of FL-NZ and FL+NZ and the FL solution will be discussed further in the following section for obtaining the scientific basis for distinguishing the location of the FL molecules between in the cage of the zeolite and on the outer surface.

Quenching at the Outermost Unit Cells. The drastic difference in the k_q values obtained between the FL-NZ dispersion and the FL+NZ dispersion should be related to the

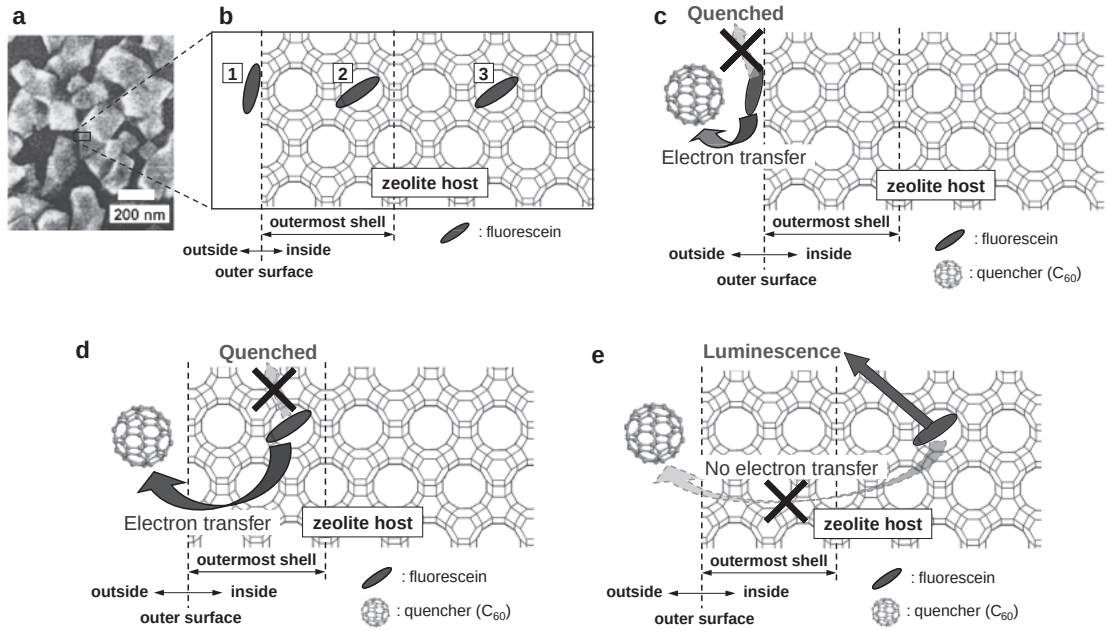

Fig. 9. Schematic images of the quenching phenomena occurring to the FL-NZ and FL+NZ systems. a) Scanning electron microscopy image of nano-sized zeolites. b) Views of the framework structure of the zeolite. Three positions for FL are shown: position 1 is a FL molecule adsorbed on the outer surface (FL_{posi1}); position 2 in a FL molecule encaged in the cage in the outermost unit cell (FL_{posi2}); position 3 is a FL molecule encaged in the cage in the inner unit cell (FL_{posi3}). c), d) In the case of FL located at the positions 1 and 2, fluorescence is quenched. e) In the case of FL locating in position 3, fluorescence is observed.

inaccessibility of C_{60} into the cage of the zeolite. Considering that the size of the open window of the zeolite is 0.7 nm compared to that of C_{60} (0.8 nm), C_{60} never enters the cage through the window. If this is the case, no quenching should be observed for the FL-NZ dispersion. However, the fluorescence was partially quenched. Why did the fluorescence intensity decrease in the FL-NZ dispersion by addition of C_{60} (Fig. 7)?

Here, we take into account FL molecules located in the outermost unit cells of the zeolite host. A cubic zeolite model with $100 \times 100 \times 100\,nm^3$ is proposed, considering the lattice constants of the FAU-type zeolite ($a = b = c = 2.4$ nm; $\alpha = \beta = \gamma = 90^\circ$). Thus, three different locations for FL molecules can be distinguished (the positions 1, 2, and 3 in Figs. 9a and 9b). Position 1 is a FL molecule adsorbed on the outer surface of zeolite (denoted as FL_{posi1}) representing FL in FL+NZ, and an excited state of this FL should be readily quenched by C_{60} due to electron transfer from FL to C_{60} (Fig. 9c). Position 2 is a FL molecule encaged in the cage in the outermost unit cell (denoted as FL_{posi2}). An excited state of FL_{posi2} could be quenched by C_{60}, because C_{60} can approach FL_{posi2} within the critical distance of the quenching. The lattice constant of FAU-type zeolite (2.4 nm), is close to the critical distance of electron transfer generally accepted (1–2 nm).[24,25] In the model of the cubic FAU-type zeolite, there are 74088 unit cells in total, and 10088 unit cells of these are classified as the outermost unit cells, corresponding to 14% of the total unit cells. Assuming that FL molecules are uniformly located in each zeolite particle, 14% of the FL molecules are located in the cages in the outermost unit cells. This value coincides to the percentage of the quenched fluorescence observed for the FL-NZ dispersion (13%) in the presence of C_{60} ($0.09\,g\,L^{-1}$). Although we have mentioned above that FL encaged in a zeolite host should not be quenched by C_{60} considering the inaccessibility of C_{60} into the cage of the zeolite, an excited state of FL_{posi2} located in the outermost unit cells could be quenched by C_{60}, resulting in the partial quenching observed for FL-NZ.

Position 3 is a FL molecule encaged in the cage in the inner unit cells (denoted as FL_{posi3}). An excited state of FL_{posi3} is never quenched by C_{60}, because C_{60} cannot approach FL_{posi3} within the critical distance for the electron transfer quenching. So, FL_{posi3} should not suffer from fluorescence quenching. Now, it is clear why partial quenching was observed for the FL-NZ dispersion and have found a basis for a new method for obtaining evidence of the encapsulation in the inner cages of the zeolite host.

As explained in Fig. 9, we have introduced three positions for FL molecules and are ready to discuss the values of k_q using this idea. We need to consider only FL_{posi2} and FL_{posi3} in explaining the quenching phenomena. The quenching phenomena of FL-NZ are expressed in the following reaction equations.

$$FL_{posi2} + FL_{posi3} + 2h\nu \rightarrow FL_{posi2}{}^* + FL_{posi3}{}^* \quad \text{(excitation)} \quad \text{(process 1)}, \tag{2}$$

$$FL_{posi2}{}^* + FL_{posi3}{}^* \rightarrow FL_{posi2} + FL_{posi3} + 2h\nu' \quad \text{(fluorescence)} \quad \text{(process 2)}, \tag{3}$$

$$FL_{posi2}{}^* + C_{60} \rightarrow FL_{posi2} + C_{60}{}^* \quad \text{(quenching)} \quad \text{(process 3)}, \tag{4}$$

$$FL_{posi3}{}^* + C_{60} \rightarrow FL_{posi3} + C_{60} + h\nu' \quad \text{(fluorescence, no quenching)} \quad \text{(process 4)}. \tag{5}$$

Only the fluorescence from FL_{posi2} (about 14% of all FL) in FL-NZ is readily quenched by C_{60} (process 3), but the fluores-

cence of FL_{posi3} is never quenched by C_{60} (process 4). Here, we ascribe the fluorescence of 86% left even after addition of C_{60} to the fluorescence of FL_{posi3}.

Let's compare the three values of k_q obtained for the FL solution, the FL-NZ dispersion, and the FL+NZ dispersion. The apparent value of k_q ($0.65\,dm^{-3}\,g\,ns^{-1}$) for the FL-NZ dispersion was smaller than that for the FL solution, because of the inability of C_{60} to enter into the zeolite cage. This value should be related to a slow quenching process of fluorescence of FL_{posi2}. Thus, the k_q value must be apparent for the FL-NZ dispersion and it should be close to zero for FL_{posi3}. At least, we can emphasize the fact that the k_q value is smaller than that for the FL solution and is much smaller than that for the FL+NZ dispersion. On the other hand, the large k_q value observed for the FL+NZ dispersion might be explained as an accumulation effect of FL molecules and C_{60} on the outer surface of the zeolite. In other words, the local concentrations of FL and C_{60} are increased due to the adsorption of these molecules on the surface.

Conclusion

We proposed a novel method for clear distinction of the location of luminescent guests in host–guest systems using a luminescence quenching. We successfully provided evidence for the encapsulation of fluorescein molecules in the cages of the zeolite host in this paper. This method is expected to be applicable to general host–guest systems by selection of a suitable quencher.

This work was supported by Research Fellowship of the Japan Society for the Promotion of Science for Young Scientists. This work was also supported in part by a Grant-in-Aid for Scientific Research on Priority Areas (417) (No. 17029038) and (460) (No. 19028048) from MEXT of the Japanese Government.

Supporting Information

Frequency domain lifetime plots for anthracene, PPO, and POPOP solutions are shown in Fig. S1. And absorption spectra of C_{60} dispersions at various C_{60} concentrations are shown in Fig. S2. Experimental procedures for the measurements of fluorescence quenching of FL solutions are also described, and the results are shown in Figs. S3, S4, S5, and S6. This material is available free of charge on the web at: http://www.csj.jp/journals/bcsj/.

References

1 D. Ishii, K. Kinbara, Y. Ishida, N. Ishii, M. Okochi, M. Yohda, T. Aida, *Nature* **2003**, *423*, 628.
2 A. Fukuoka, H. Miyata, K. Kuroda, *Chem. Commun.* **2003**, 284.
3 T. Nakashima, T. Kawai, *Chem. Commun.* **2005**, 1643.
4 K. Ishikawa, T. Okubo, *J. Appl. Phys.* **2005**, *98*, 043502.
5 C. M. Niemeyer, *Angew. Chem., Int. Ed.* **2003**, *42*, 5796.
6 N. J. Turro, *Chem. Commun.* **2002**, 2279.
7 S. J. Dalgarno, S. A. Tucker, D. B. Bassil, J. L. Atwood, *Science* **2005**, *309*, 2037.
8 Y. Inoue, M. Okamoto, J. Morimoto, *Jpn. J. Appl. Phys.* **2006**, *45*, 4128.
9 Y. Wada, M. Sato, Y. Tsukahara, *Angew. Chem., Int. Ed.* **2006**, *45*, 1925.
10 T. Baba, K. Inazu, *Chem. Lett.* **2006**, *35*, 142.
11 T. Beutel, B.-L. Su, *Chem. Phys. Lett.* **2005**, *416*, 51.
12 D. Han, A. J. Woo, I. Nam, S. B. Hong, *J. Phys. Chem. B* **2002**, *106*, 6206.
13 M. J. Truitt, S. S. Toporek, R. Rovira-Hernandez, K. Hatcher, J. L. White, *J. Am. Chem. Soc.* **2004**, *126*, 11144.
14 F. L. Cozens, M. L. Cano, H. García, N. P. Schepp, *J. Am. Chem. Soc.* **1998**, *120*, 5667.
15 M. Salavati-Niasari, *Chem. Lett.* **2005**, *34*, 1444.
16 C. Lai, B. G. Trewyn, D. M. Jeftinija, K. Jeftinija, S. Xu, S. Jeftinija, V. S.-Y. Lin, *J. Am. Chem. Soc.* **2003**, *125*, 4451.
17 Y. Lin, A. Böker, J. He, K. Sill, H. Xiang, C. Abetz, X. Li, J. Wang, T. Emrick, S. Long, Q. Wang, A. Balazs, T. P. Russel, *Nature* **2005**, *434*, 55.
18 P. Simoncic, T. Armbruster, P. Pattison, *J. Phys. Chem. B* **2004**, *108*, 17352.
19 M. Koshino, T. Tanaka, N. Solin, K. Suenaga, H. Isobe, E. Nakamura, *Science* **2007**, *316*, 853.
20 M. Miyauchi, A. Harada, *J. Am. Chem. Soc.* **2004**, *126*, 11418.
21 A. Robertson, M. Ikeda, M. Takeuchi, S. Shinkai, *Bull. Chem. Soc. Jpn.* **2001**, *74*, 883.
22 V. Ramamurthy, D. R. Sanderson, D. F. Eaton, *J. Am. Chem. Soc.* **1993**, *115*, 10438.
23 T. Ban, D. Brühwiler, G. Calzaferri, *J. Phys. Chem. B* **2004**, *108*, 16348.
24 H. Ohkita, T. Ogi, R. Kinoshita, S. Ito, M. Yamamoto, *Polymer* **2002**, *43*, 3571.
25 K. Nagai, T. Nishijima, N. Takamiya, M. Tada, M. Kaneko, *J. Photochem. Photobiol., A* **1995**, *92*, 47.
26 T. Förster, *Ann. Phys.* **1948**, *437*, 55.
27 D. L. Dexter, *J. Chem. Phys.* **1953**, *21*, 836.
28 J. R. Lakowicz, *Principles of Fluorescence Spectroscopy*, 3rd ed., Spribger, New York, **2006**, p. 279.
29 B. Jing, D. Zhang, D. Zhu, *Tetrahedron Lett.* **2000**, *41*, 8559.
30 S. Mintova, N. H. Olson, T. Bein, *Angew. Chem., Int. Ed.* **1999**, *38*, 3201.
31 M. N. Chrétien, B. Shen, H. García, A. M. English, J. C. Scaiano, *Photochem. Photobiol.* **2004**, *80*, 434.
32 J. R. Lakowicz, *Principles of Fluorescence Spectroscopy*, 3rd ed., Spribger, New York, **2006**, pp. 157–199.
33 J. R. Lakowicz, *Principles of Fluorescence Spectroscopy*, 3rd ed., Spribger, New York, **2006**, pp. 883–887.
34 M. Arik, N. Çelebi, Y. Onganer, *J. Photochem. Photobiol., A* **2005**, *170*, 105.
35 Baeyer, *Ber.* **1871**, *4*, 555.
36 L. Wang, Y. Shao, J. Zhang, M. Anpo, *Opt. Mater.* **2006**, *28*, 1232.
37 O. Stern, M. Volmer, *Z. Phys.* **1919**, *20*, 183.